RSC Advances

ROYAL SOCIETY OF CHEMISTRY

www.rsc.org/advances

Table of contents entry

Four new PTP1B inhibitors were isolated from *Glycyrrhiza uralensis*, and the absolute configuration of 2,3-dihydro-2,3,3-trimethylbenzofurans was firstly unambiguously established.

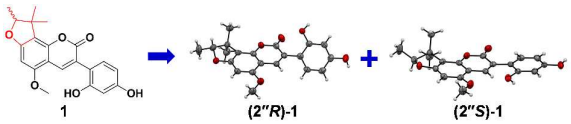

Enantiomeric 3-arylcoumarins and 2-arylcoumarones from the roots of *Glycyrrhiza uralensis* as protein tyrosine phosphatase 1B (PTP1B) inhibitors

Shuai Ji,[a] Xue Qiao,[a] Zi-wei Li,[a] Yong-rui Wang,[a] Si-wang Yu,[a] Wen-fei Liang,[a] Xiong-hao Lin[a] and Min Ye[*a,b]

[a] *State Key Laboratory of Natural and Biomimetic Drugs, School of Pharmaceutical Sciences, Peking University, 38 Xueyuan Road, Beijing 100191, China*

[b] *State Key Laboratory of Drug Research, Shanghai Institute of Materia Medica, Chinese Academy of Sciences, 555 Zuchongzhi Road, Shanghai 201203, China*

[*] Corresponding author. State Key Laboratory of Natural and Biomimetic Drugs, School of Pharmaceutical Sciences, Peking University, 38 Xueyuan Road, Beijing 100191, China. Tel.: +86 10 82801516. Fax: +86 10 82802024. E-mail address: yemin@bjmu.edu.cn (M. Ye).

Abstract

Glycyfuranocoumarin A–C (**1**–**3**), three 3-arylcoumarins, and glycyfuranocoumarone A (**4**), one 2-arylcoumarone, were isolated in the racemic form from the roots of *Glycyrrhiza uralensis*. Their structures were elucidated by NMR, 2D NMR and HRESIMS data analyses. All the structures contain a 2,3-dihydro-2,3,3-trimethylbenzofuran ring. Chiral HPLC was used to obtain the optically pure enantiomers, (2″*R*)-**1** and (2″*S*)-**1**. Their absolute configurations were determined by X-ray crystallography. This is the first unambiguous determination of the absolute configuration of 2,3-dihydro-2,3,3-trimethylbenzofurans. (2″*R*)-**1** and (2″*S*)-**1**, as well as **2**–**4**, exhibited significant inhibitory activities against protein tyrosine phosphatase 1B (PTP1B). Among them, **4** showed IC_{50} of 2.2 μM.

Introduction

Diabetes mellitus is a major metabolic syndrome affecting human health. It could lead to a series of complications like blindness, renal diseases, and cardiovascular diseases.[1] Protein tyrosine phosphatase 1B (PTP1B) plays a critical role in the negative regulation of insulin and leptin signaling pathways.[2,3] Thus, PTP1B inhibition has been considered as a potential therapeutic approach against type 2 diabetes.[4] Although a number of PTP1B inhibitors have been reported, majority of them suffer from poor pharmacokinetic properties and low enzyme selectivity. Therefore, to discover new potent PTP1B inhibitors is still of great significance.[5]

Glycyrrhiza uralensis Fisch. is the major source for licorice (Gan-Cao in Chinese), one of the most popular herbal medicines worldwide. It is recorded in the pharmacopoeia of China, Japan, Europe, and the United States.[6,7] *G. uralensis* has been reported to exhibit significant anti-diabetic activities, and flavonoids and coumarins are considered be the major bioactive constituents.[8-11] In this work, we report four new PTP1B inhibitors isolated from *G. uralensis*, namely glycyfuranocoumarin A–C (**1**–**3**) and glycyfuranocoumarone A (**4**). Furthermore, the racemic mixture of **1** was separated by chiral HPLC, and the absolute configurations of the 2,3-dihydro-2,3,3-trimethylbenzofuran ring for the enantiomers were established by X-ray crystallography. The cytotoxic activities of **1**–**4** against human cancer cell lines (SW480, HepG2, and A549) were also evaluated.

Results and discussion

The dried roots of *Glycyrrhiza uralensis* (35 kg) were extracted with 95% and 70% EtOH, and the combined extract was successively extracted with EtOAc and *n*-BuOH. The EtOAc extract was separated by silica gel, ODS C_{18}, Sephadex LH-20 and semi-preparative RP-HPLC to afford glycyfuranocoumarin A–C (**1**–**3**) and glycyfuranocoumarone A (**4**) (Fig. 1). Their structures were identified on the basis of extensive NMR and MS data analyses.

The molecular formula of compound **1** was established as $C_{21}H_{20}O_6$ by its HRESIMS spectrum ($[M-H]^-$ *m/z* 367.1166, calcd for $C_{21}H_{19}O_6$, 367.1176). The UV spectrum with maximal absorptions at 267 nm and 359 nm was typical for a 3-arylcoumarin skeleton,[12] and the ^{1}H NMR spectrum (Table 1) showed a characteristic singlet at δ_H 7.86 (1H, s) corresponding to H-4.[12] The remaining proton signals indicated the presence of an aromatic ABX system [δ_H 7.05 (1H, d, J = 8.4 Hz), 6.25 (1H, dd, J = 2.0, 8.4 Hz) and 6.35 (1H, d, J = 2.0 Hz)], an aromatic singlet at δ_H 6.49 (1H, s), a methoxyl group at δ_H 3.85 (3H, s), two phenolic hydroxyl groups at δ_H 9.37 (1H, s) and 9.33 (1H, s), and a 2,3-dihydro-2,3,3-trimethylbenzofuran ring [δ_H 1.21 (3H, s), 1.47 (3H, s), 1.35 (3H, d, J = 6.8 Hz) and 4.52 (1H, q, J = 6.8 Hz)].[13] The ^{13}C NMR spectrum of **1** exhibited 21 carbon signals corresponding to five aromatic methines at δ_C 136.6, 131.4, 106.2, 102.6 and 90.5, nine aromatic quaternary carbons at δ_C 162.0, 158.3, 156.8, 155.9, 150.7, 119.1, 113.6, 113.3 and 103.6, a lactone carbonyl group at δ_C 159.6, a methoxyl group at δ_C 56.4, and the

2,3-dihydro-2,3,3-trimethylbenzofuran ring [δ_C 21.1 (CH_3), 25.3 (CH_3), 14.1 (CH_3), 90.0 (CH) and 43.2 (C)].

The aromatic ABX system was assigned to ring B due to the HMBC correlation between H-6′ (δ_H 7.05) and C-3 (δ_C 119.1) (Fig. 2). The two hydroxyl groups at C-2′ and C-4′ were determined by the HMBC correlations of 2′-OH (δ_H 9.33)/C-1′ (δ_C 113.6), C-2′ (δ_C 155.9), C-3′ (δ_C 102.6), and 4′-OH (δ_H 9.37)/C-3′, C-4′ (δ_C 158.3), C-5′ (δ_C 106.2), respectively. The HMBC correlations of H-5″ (δ_H 1.21), H-6″ (δ_H 1.47)/C-8 (δ_C 113.3), H-2″ (δ_H 4.52)/C-7 (δ_C 162.0), and H-4 (δ_H 7.86), H-6 (δ_H 6.49)/C-5 (δ_C 156.8) indicated that the 2,3-dihydro-2,3,3-trimethylfuran ring was connected to C-7 and C-8 of the 3-arylcoumarin skeleton. Location of the methoxyl group was determined by its HMBC correlation with C-5 (δ_C 156.8). Thus, the planar structure of **1** was established as shown in Fig. 1, and was named as glycyfuranocoumarin A.

Initially, we intended to determine the absolute configuration of the 2,3-dihydro-2,3,3-trimethylfuran ring in **1** by comparing the experimental and calculated electronic circular dichroism (ECD) spectra.[14] The calculated ECD spectra of (2″*R*)-**1** and (2″*S*)-**1** were obtained by time-dependent density functional theory (TDDFT) at the B3LYP/6-31G* level in the MeCN solution with the IEFPCM model.[15] They showed remarkably opposite Cotton effects. However, the experimental ECD spectrum of **1** showed a nearly straight line, which indicated that **1**

might be a raceme (Fig. 3). After repeated attempts, we obtained its single crystals from the MeOH-H_2O (80:20, *v*/*v*) solution. The X-ray diffraction experiment (Cu Kα) confirmed that **1** was a raceme with the co-crystallization of (2″*R*)-**1** and (2″*S*)-**1** (Fig. 4).

In order to obtain the optically pure enantiomers, we initially tried to separate the racemic **1** by analytical supercritical fluid chromatography (SFC), which was a rapid and efficient approach for chiral resolution.[16] As expected (Fig. 5), (2″*R*)-**1** and (2″*S*)-**1** could be separated on a Chiralcel IC-3 column (2.1 × 150 mm, 3 μm, Daicel) eluted with 25–30% MeOH (0–10 min) in CO_2 at 2 mL/min. However, the low resolution made it difficult to obtain the pure enantiomers. We further tested chiral HPLC,[17] and found that the normal-phase Chiralcel OZ-H column (4.6 × 250 mm, 5 μm, Daicel) could efficiently separate (2″*R*)-**1** (t_R=12.9 min) and (2″*S*)-**1** (t_R=9.2 min), eluted with *n*-hexane-isopropanol (75:25, *v*/*v*) at 1 mL/min (Fig. 6). Therefore, a 14-min analytical-scale method was established to obtain 2.5 mg of (2″*R*)-**1** and 4.5 mg of (2″*S*)-**1**. They showed opposite optical activities of $[\alpha]_D^{25}$ +0.3 (*c* 0.01, MeOH) and $[\alpha]_D^{25}$ -0.4 (*c* 0.01, MeOH), respectively. To fully establish the absolute configuration of the two enantiomers, we obtained their respective single crystals from MeOH-H_2O solution (80:20 for (2″*R*)-**1**, and 90:10 for (2″*S*)-**1**, *v*/*v*) through a series of attempts. The X-ray diffraction experiments (Cu Kα) unambiguously determined the stereochemistry of (2″*R*)-**1** and (2″*S*)-**1** (Fig. 4). On the other hand, we also recorded their ECD spectra separately. As shown in Fig. 3, the calculated ECD

spectra for (2″*R*)-**1** and (2″*S*)-**1** agreed well with their respective experimental spectra. This result indicated that ECD calculations could be an efficient approach to establish the absolute configuration of the 2,3-dihydro-2,3,3-trimethylbenzofuran ring.

The molecular formula of compound **2** was determined to be $C_{21}H_{20}O_7$ on the basis of its HRESIMS spectrum ([M-H]$^-$ *m/z* 383.1123, calcd for $C_{21}H_{19}O_7$, 383.1125). Its 1D and 2D NMR spectra were very similar to those of **1**, and the main differences were in the 2,3-dihydro-2,3,3-trimethylbenzofuran ring. The methyl group for C-4″ (δ_C 14.1) of **1** disappeared, and an oxygenated methylene at δ_C 59.6 appeared in **2**. In accordance, the signal for H-4″ shifted downfield from δ_H 1.35 (3H, d, J = 6.8 Hz) in **1** to δ_H 3.75 (2H, m) in **2**. Furthermore, a hydroxyl group at δ_H 4.99 (1H, br s) appeared in the ^{1}H NMR spectrum of **2**. These signals indicated that the methyl group in **1** was replaced by a hydroxymethyl group in **2**, which was confirmed by the HMBC correlations of H-4″ (δ_H 3.75)/C-2″ (δ_C 93.9) and C-3″ (δ_C 42.7). Therefore, the planar structure of **2** was identified as shown in Fig. 1, and was named as glycyfuranocoumarin B.

Compound **3** exhibited a pseudomolecular ion in the HRESIMS spectrum at *m/z* 365.1009 ([M-H]$^-$, calcd for $C_{21}H_{17}O_6$, 365.1019), corresponding to the molecular formula of $C_{21}H_{18}O_6$, two fewer protons than **1**. The 1D and 2D NMR spectra of **3** were also very similar to those of **1**, and the main differences were in C-4. The olefinic carbon for C-4 (δ_C 136.6) in **1** disappeared, and an oxygenated olefinic carbon

at δ_C 157.1 appeared in **3**. In accordance, the H-4 signal at δ_H 7.86 for **1** also disappeared. These evidences indicated that a hydroxyl group was introduced to C-4 in **3**. However, the molecular formula of **3** was calculated to be $C_{21}H_{20}O_7$, which had one more molecule of H_2O than the measured result ($C_{21}H_{18}O_6$). By careful analysis, we observed only one hydroxyl group (δ_H 9.99) in the ^{1}H NMR spectrum of **3**, one fewer than that of **1**. Based on the above evidences, it could be deduced that 4-OH and 2′-OH formed an ether linkage. Thus, the planar structure of **3** was identified as shown in Fig. 1, and was named as glycyfuranocoumarin C.

Compound **4** had a molecular formula of $C_{20}H_{20}O_5$ according to its HRESIMS spectrum ($[M-H]^-$ *m/z* 339.1217, calcd for $C_{20}H_{19}O_5$, 339.1227). Its UV spectrum showed maximum absorptions at 252 nm and 321 nm, corresponding to a 2-arylcoumarone skeleton. The ^{1}H NMR spectrum showed a characteristic singlet at δ_H 7.03 (1H, s) corresponding to H-3.[18] The remaining proton signals included an aromatic ABX system [δ_H 7.58 (1H, d, *J* = 8.4 Hz), 6.37 (1H, dd, *J* = 2.0, 8.4 Hz) and 6.45 (1H, d, *J* = 2.0 Hz)], a single aromatic proton at δ_H 6.31 (1H, s), a methoxyl group at δ_H 3.82 (3H, s), two phenolic hydroxyl groups at δ_H 10.15 (1H, br s) and 9.54 (1H, br s), and a 2,3-dihydro-2,3,3-trimethylbenzofuran ring [δ_H 1.21 (3H, s), 1.51 (3H, s), 1.34 (3H, d, *J* = 6.8 Hz) and 4.45 (1H, q, *J* = 6.8 Hz)]. The 1,2,4-substituted aromatic ABX system was determined to be at ring C because of the HMBC correlations of H-6′ (δ_H 7.58)/C-2 (δ_C 150.2), C-2′ (δ_C 155.4), C-4′ (δ_C 158.1) and H-5′ (δ_H 6.37)/C-1′ (δ_C 109.0), C-3′ (δ_C 102.9). The methoxyl group was connected to C-4

(δ_C 152.3), as evidenced by its HMBC correlation with C-4 and the HMBC correlation of H-3 (δ_H 7.03)/C-4. The single aromatic proton at δ_H 6.31 (1H, s) was assigned to H-5 based on its HMBC correlations with C-4 (δ_C 152.3), C-6 (δ_C 156.7), C-7 (δ_C 110.8) and C-9 (δ_C 113.4), which was confirmed by the NOE enhancement between H-5 (δ_H 6.31) and 4-OCH_3 (δ_H 3.82) (Fig. 2). In addition, the HMBC correlations of H-5″ (δ_H 1.21), H-6″ (δ_H 1.51)/C-7 (δ_C 110.8), as well as H-2″ (δ_H 4.45)/C-6 (δ_C 156.7), C-7 (δ_C 110.8) indicated that the 2,3-dihydro-2,3,3-trimethylbenzofuran ring was connected to C-6 and C-7 of the 2-arylcoumarone skeleton. These deductions established the planar structure of **4** as shown in Fig. 1. It was named as glycyfuranocoumarone A.

Because of the weak optical activities of compound **2** ($[\alpha]_D^{25}$ -0.004 (*c* 0.01, MeOH)), **3** ($[\alpha]_D^{25}$ -0.002 (*c* -0.01, MeOH)) and **4** ($[\alpha]_D^{25}$ +0.001 (*c* 0.01, MeOH)), as well as the common 2,3-dihydro-2,3,3-trimethylbenzofuran ring, we speculated that all of them were racemes. This was confirmed by SFC analyses. Through a series of attempts, the three pairs of enantiomers were successfully separated on different chiral columns within 20 min at different conditions (Fig. 5). Regretfully, it was difficult to prepare the optically pure enantiomers of **2**–**4** due to their very limited amounts.

To the best of our knowledge, only a few natural compounds with a 2,3-dihydro-2,3,3-trimethylbenzofuran ring have been reported, thus far.[12,19] Moreover, the absolute configuration for the dihydrofuran ring has never been

established. Enantiomers (2″*R*)-**1** and (2″*S*)-**1** represented the first pure optical forms of the 2,3-dihydro-2,3,3-trimethylbenzofuran ring with unambiguously established absolute configuration. They showed opposite optical activities and ECD spectra, which could be used to rapidly and efficiently determine the absolute configuration of similar compounds with a 2,3-dihydro-2,3,3-trimethylbenzofuran ring. According to the HPLC chromatograms shown in Fig. 5, the *R*/*S* ratio for all the four pairs of enantiomers was approximately 1:1. This result suggested the 2,3-dihydro-2,3,3-trimethylbenzofuran ring may occur in the form of raceme in the nature. On the other hand, compound **4** obtained in this study was the first 2-arylcoumarone skeleton with the 2,3-dihydro-2,3,3-trimethylbenzofuran ring.

The inhibitory activities of (2″*R*)-**1**, (2″*S*)-**1** and **2**–**4** against protein tyrosine phosphatase 1B (PTP1B) were evaluated using *p*-nitrophenyl phosphate (*p*NPP) as the substrate according to previously described methods.[3,4] The known PTP1B inhibitor, ursolic acid (IC_{50} = 6.2 μM), was used as the positive control.[20] As shown in Table 2, (2″*R*)-**1**, (2″*S*)-**1**, **2** and **3** exhibited noticeable PTP1B inhibition with IC_{50} values ranging from 10.3 to 13.6 μM. Compound **4** showed significant inhibition with IC_{50} values of 2.2 μM, which was more potent than the positive control. In addition, (2″*R*)-**1** and (2″*S*)-**1** showed similar inhibitory activities with IC_{50} values of 12.1 μM and 13.6 μM, respectively, suggesting that the absolute configuration of C-2″ hardly affected the inhibitory activity.

The cytotoxicities of these five compounds against three human cancer cell lines, namely human colorectal adenocarcinoma cell line (SW480), human hepatocellular liver carcinoma cell line (HepG2) and human alveolar adenocarcinoma cell line (A549) were also evaluated. As the same as PTP1B inhibitory activity, compound **4** showed the most potent cytotoxic activity with the IC_{50} values of 4.4 μM (SW480), 6.7 μM (HepG2) and 13.7 μM (A549). Interestingly, (2″*R*)-**1** exhibited remarkably higher cytotoxic activities than (2″*S*)-**1** (Table 2). For example, (2″*R*)-**1** could inhibit SW480 cell viability with an IC_{50} value of 11.6 μM, whereas (2″*S*)-**1** only showed an IC_{50} value of above 40 μM (Fig. S1). Similarly, (2″*R*)-**1** exhibited stronger cytotoxic activities than (2″*S*)-**1** for HepG2 and A549 cells (Fig. S2 and Fig. S3).

Conclusions

In conclusion, three 3-arylcoumarins (**1**–**3**) and one 2-arylcoumarone (**4**) were isolated from the roots of *Glycyrrhiza uralensis* in the racemic form. Their structures were elucidated by extensive spectroscopic analysis, and all of them contain a 2,3-dihydro-2,3,3-trimethylbenzofuran ring. Compound **1** was separated by chiral HPLC to yield (2″*R*)-**1** and (2″*S*)-**1**, whose absolute configuration was unambiguously established by X-ray crystallography and ECD spectra. This is the first unambiguous determination of the absolute configuration of 2,3-dihydro-2,3,3-trimethylbenzofurans. All of (2″*R*)-**1**, (2″*S*)-**1** and racemic **2**–**4** exhibited good inhibitory activities against PTP1B, especially **4** (IC_{50} = 2.2 μM). Interestingly, (2″*R*)-**1** showed remarkably higher cytotoxic activities than (2″*S*)-**1** against human cancer cell lines (SW480,

HepG2, and A549).

Experimental section

General Experimental Procedures

Optical rotations were measured on a Rudolph Research Autopol III automatic polarimeter. IR spectra were recorded as KBr disks on a Nicolet NEXUS-470 FT-IR spectrometer. UV spectra were measured on a Cary 300 Bio UV−visible spectrophotometer. NMR spectra were recorded at 400 MHz for ^{1}H and 100 MHz for ^{13}C on a Bruker AVANCE III-400 spectrometer in DMSO-d_6 with TMS as the reference. ECD spectra were recorded on a JASCO J-810 CD spectrometer. HRESIMS data were performed on a Bruker APEX IV FT-MS spectrometer. TLC was carried out on precoated silica gel GF_{254} plates (Qingdao Marine Chemical Inc., China). Spots were visualized under UV light (365 nm). Open column chromatography was performed using silica gel (200−300 mesh, Qingdao Marine Chemical Inc., China), ODS C_{18} (DAISO Company, Japan), and Sephadex LH-20 (GE Healthcare Bio-Science AB, USA). Semi-preparative HPLC was performed on an Agilent 1200 instrument equipped with a ZORBAX SB C_{18} column (250 mm × 9.4 mm, i.d. 5 μm, Agilent, USA). Chiral HPLC was performed on a Shimadzu LC-20A instrument equipped with a normal-phase Chiralcel OZ-H column (4.6 × 250 mm, i.d. 5 μm, Daicel Industries, Japan.)

Plant Materials

Dried roots of *G. uralensis* Fisch. were collected in September 2012 in Chifeng City, Inner Mongolia Autonomous Region, China. The plant was identified by the authors. A voucher specimen (No. GC-201209) was deposited at the School of Pharmaceutical Sciences, Peking University, Beijing, China.

Extraction and Isolation

The dried material (35 kg) was powdered and extracted with 95% (90 L × 2 h × 2) and 70% EtOH (90 L × 2 h × 1) under reflux. After concentration *in vacuo*, the extract (10 L) was dispersed in H_2O and successively extracted with EtOAc and *n*-BuOH. The EtOAc extract (1280 g) was chromatographed over silica gel using petroleum ether/EtOAc (1:0 to 1:1, v/v) as the eluent to produce fractions A−H. Fraction E was chromatographed over silica gel using $CHCl_3$/MeOH (1:0 to 2:1, v/v) as the eluent to produce fractions EA−EE. Fraction EC was further purified over Sephadex LH-20 (MeOH) and semi-preparative HPLC (75% MeCN-H_2O) to yield compound **1** (9.5 mg). Compound **1** was separated into (2″*R*)-**1** (2.5 mg) and (2″*S*)-**1** (4.5 mg) by chiral HPLC with *n*-hexane-isopropanol (75:25, v/v, 1 mL/min) as the eluent. Fraction EF was fractionated by silica gel eluted with $CHCl_3$/MeOH (1:0 to 2:1, v/v), followed by Sephadex LH-20 (MeOH) and semi-preparative HPLC (79% MeCN-H_2O) to yield **3** (2.1 mg) and **4** (1.9 mg). Fraction D were fractionated by an ODS C_{18} column eluted with MeOH/H_2O (50 to 90%, v/v) to obtain fraction DB, which was further purified over semi-preparative HPLC (71% MeCN-H_2O) to yield compound **2** (3.2 mg).

Glycyfuranocoumarin A (**1**): pale yellow lamellar crystals (MeOH/H_2O, 80:20, v/v); UV (MeOH) λ_{max} (log ε) 266 (3.78), 362 (4.54) nm; IR ν_{max} = 2989, 1765, 1599, 1456, 1377, 1243, 1056 cm^{-1}; for ^1H and ^{13}C NMR data, see Table 1; HRESIMS *m/z* 367.1166 $[M-H]^-$, calcd for $C_{21}H_{19}O_6$, 367.1176.

(2″*R*)-**1**: pale yellow lamellar crystals (MeOH/H_2O, 80:20, v/v); mp 295–298 ℃; $[\alpha]_D^{25}$ +0.3 (*c* 0.01, MeOH); ECD (MeCN) λ_{max} ($\Delta\varepsilon$) 200 (+8.96), 260 (+2.72) nm.

(2″*S*)-**1**: pale yellow lamellar crystals (MeOH/H_2O, 90:10, v/v); mp 294–297 ℃; $[\alpha]_D^{25}$ -0.4 (*c* 0.01, MeOH); ECD (MeCN) λ_{max} ($\Delta\varepsilon$) 212 (-7.39), 274 (-1.16) nm.

Crystal data for racemic **1**: $C_{21}H_{20}O_6$, *M* =368.37, orthorhombic, *a* = 9.33933(18) Å, *b* = 19.7504(4) Å, *c* = 9.61969(17) Å, *V* = 1774.40(6) $Å^3$, *T* = 180.01(10) K, space group $P2_12_12_1$ (no. 19), *Z* = 4, μ(Cu Kα) = 0.840 mm^{-1}, 29236 reflections measured, 3570 unique (R_{int} = 0.0456) which were used in all calculations. The final wR_2 was 0.1025 (all data). Flack parameter = 0.10 (6).

Crystal data for (2″*R*)-**1**: $C_{21}H_{20}O_6$, *M* =368.37, orthorhombic, *a* = 9.3372(5) Å, *b* = 9.6286(3) Å, *c* = 19.5494(6) Å, *U* = 1757.57(12) $Å^3$, *T* = 104.3, space group $P2_12_12_1$ (no. 19), *Z* = 4, μ(Cu Kα) = 0.848, 5776 reflections measured, 3325 unique (R_{int} = 0.0209) which were used in all calculations. The final $wR(F_2)$ was 0.0879 (all data). Flack parameter = -0.03 (16).

Crystal data for (2″*S*)-**1**: $C_{21}H_{20}O_6$, *M* =368.37, orthorhombic, *a* = 9.3355(3) Å, *b* = 9.6307(3) Å, *c* = 19.5386(3) Å, *U* = 1756.67(9) $Å^3$, *T* = 100.8, space group $P2_12_12_1$ (no. 19), *Z* = 4, μ(Cu Kα) = 0.848, 5784 reflections measured, 3321 unique (R_{int} = 0.0280) which were used in all calculations. The final $wR(F_2)$ was

0.0908 (all data). Flack parameter = -0.04 (16). Crystallographic data for racemic **1**, (2″*R*)-**1** and (2″*S*)-**1** have been deposited at the Cambridge Crystallographic Data Centre, with deposition Nos. CCDC 1040681, CCDC 1040577 and CCDC 1040660, respectively.

Glycyfuranocoumarin B (**2**): pale yellow powder; $[\alpha]_D^{25}$ -0.004 (*c* 0.01, MeOH); UV (MeOH) λ_{max} (log ε) 267 (3.89), 362 (4.21) nm; IR ν_{max} = 3403, 2926, 1695, 1601, 1472, 1452, 1296, 1106 cm^{-1}; for ^1H and ^{13}C NMR data, see Table 1; HRESIMS *m/z* 383.1123 $[M-H]^-$, calcd for $C_{21}H_{19}O_7$, 383.1125.

Glycyfuranocoumarin C (**3**): pale yellow powder; $[\alpha]_D^{25}$ -0.002 (*c* 0.01, MeOH); UV (MeOH) λ_{max} (log ε) 252 (2.68), 347 (4.76) nm; IR ν_{max} = 3433, 2923, 1703, 1616, 1439, 1376, 1162, 1084 cm^{-1}; for ^1H and ^{13}C NMR data, see Table 1; HRESIMS *m/z* 365.1009 $[M-H]^-$, calcd for $C_{21}H_{17}O_6$, 365.1019.

Glycyfuranocoumarone A (**4**): pale yellow powder; $[\alpha]_D^{25}$ +0.001 (*c* 0.01, MeOH); UV (MeOH) λ_{max} (log ε) 251 (2.41), 321 (3.68) nm; IR ν_{max} = 3365, 2988, 1765, 1623, 1377, 1243, 1053 cm^{-1}; for ^1H and ^{13}C NMR data, see Table 1; HRESIMS *m/z* 339.1217 $[M-H]^-$, calcd for $C_{20}H_{19}O_5$, 339.1227.

Analytical supercritical fluid chromatography (SFC)

SFC analysis was performed on an Agilent 1260 Infinity analytical SFC system consisting of an SFC Fusion™A5 module, a modified 1260 Infinity LC system, a degasser, an SFC binary pump, an SFC autosampler, a thermostated column compartment, and a diode array detector with a high pressure SFC flow cell. The

following analytical columns were used: Chiralcel OJ-H (4.6 × 250 mm, 5 μm, Daicel Industries, Tokyo, Japan), Chiralpak IC-3 (2.1 × 150 mm, 3 μm, Daicel) and Chiralpak AD-H (4.6 × 250 mm, 5 μm, Daicel). The back pressure was maintained at 120 bar, and the column temperature was 40 ℃. An aliquot of 5 μL sample was injected for analysis. Compound **1** was separated on Chiralpak IC-3 (0–10 min, 25–30% MeOH in CO_2, *v*/*v*, 2 mL/min). Compound **2** and **3** were separated on Chiralcel OJ-H (0–15 min, 5–15%; 15–20 min, 15–20% MeOH in CO_2, *v*/*v*, 3 mL/min). Compound **4** was separated on Chiralpak AD-H (0–20 min, 10–30% MeOH in CO_2, *v*/*v*, 2 mL/min). Data were processed by Openlab CDS Chemstation C.01.03 software.

ECD Calculations

A preliminary conformational search was performed in SYBYL-X 1.1 using the random search method with the MMFF94 force field.[15] The conformers were successively optimized using the semi-empirical method at the AM1 level and the density functional theory (DFT) method at the B3LYP/6-31G* level. The stable conformers with populations greater than 1% and without imaginary frequencies were submitted to ECD calculation by the TDDFT [B3LYP/6-31G*] method. Considering solvent effects on the calculated ECD spectra, we took the IEFPCM model in MeCN. ECD spectra of different conformers were simulated using SpecDis with a halfbandwidth of 0.4 eV.[21] The final ECD spectra were generated according to the Boltzmann-calculated distribution of each conformer. The calculated ECD spectra were compared with the experimental data. All the calculations have been performed

with the Gaussian 09 program package.[22]

Inhibitory effects of protein tyrosine phosphatase 1B (PTP1B)

The ability of all the isolated compounds to inhibit protein tyrosine phosphatase 1B (PTP1B) was studied by a previously described method.[3,4] Recombinant human PTP1B was purchased from Sigma-Aldrich (MO, USA). For the inhibition assay, compounds at different concentrations (1 μL in DMSO) were added to a reaction mixture containing PTP1B enzyme (0.1 μg), 99 μL of reaction buffer [50 mM HEPES (pH 7.2), 1 mM EDTA and 5 mM dithiothreitol (DTT)] and 100 μL of 4 mM *p*-nitrophenyl phosphate (*p*NPP). The reaction mixture (200 μL) was incubated at 37 ℃ for 30 min and then quenched by adding 10 μL of 10 N NaOH. The hydrolysis of *p*NPP was determined by measuring the absorbance at 405 nm. The non-enzymatic hydrolysis of 2 mM *p*NPP was corrected by measuring the increase in absorbance at 405 nm obtained in the absence of PTP1B enzyme. Ursolic acid was used as the positive control. All the experiments were performed in three independent replicates.

Cytotoxic activity evaluation

The cytotoxicities of all the isolated compounds against human colorectal adenocarcinoma cell line (SW480), human hepatocellular liver carcinoma cell line (HepG2) and human alveolar adenocarcinoma cell line (A549) were determined using the MTS assay. Briefly, SW480 cells were cultured at 37 ℃ in a humidified 5% CO_2 atmosphere in RPMI1640 medium (HepG2 cells in MEM medium and A549 in

DMEM medium) supplemented with 10% fetal bovine serum and 1×penicillin-streptomycin solution. The cells were seeded at 5×10^3 cells/well in 96-well plates and cultured overnight. Compounds at different concentrations were then added into the culture, and incubated for further 24 h. Cell viability was measured by MTS assay following the manufacturer's protocol (Promega, Madison, WI, USA). All the experiments were performed in three independent replicates.

Acknowledgments

This work was supported by National Natural Science Foundation of China (No. 81173644, No. 81222054), the Program for New Century Excellent Talents in University from Chinese Ministry of Education (No. NCET-11-0019), and the State Key Laboratory of Drug Research. We wish to thank Analytical Center of Beijing University of Chemical Technology for the kind help with crystal structure analysis. We also thank Dr. Bing Yang (Daicel Beijing Office) for his technical help to purify the enantiomers, and Drs. Rong An, Lang Li and Ying Meng (Agilent Technologies) for their technical help in SFC analyses.

References

1 (a) P. Zhang, X. Zhang, J. Brown, D. Vistisen, R. Sicree, J. Shaw and G. Nichols, *Diabetes Res. Clin. Pract.*, 2010, **87**, 293−301. (b) K. Nicholas, *FEBS Lett.*, 2003, **546**, 140−148.

2 T. O. Johnson, J. Ermolieff and M. R. Jirousek, *Nat. Rev. Drug Discov.*, 2002, **1**,

696−709.

3 M. Elchebly, *Science*, 1999, **283**, 1544−1548.

4 S. Zhang and Z. Y. Zhang, Drug Discov. Today, 2007, **12**, 373−381.

5 A. P. Combs, *J. Med. Chem.*, 2010, **53**, 2333−2344.

6 Commission of Flora of China, *Flora of China*, Chinese Science Press, Beijing, 1998, vol. **42**, pp. 168.

7 Q. Y. Zhang and M. Ye, *J. Chromatogr. A*, 2009, **1216**, 1954−1969.

8 R. Gaur, K. S. Yadav, R. K. Verma, N. P. Yadav and R. S. Bhakuni, *Phytomedicine*, 2014, **21**, 415−422.

9 L. Feng, M. Zhu, M. Zhang, R. Wang, X. Tan, J. Song, S. Ding, X. Jia and S. Hu, *J. ethnopharmacol*. 2013, **148**, 27−36.

10 W. Li, S. Li, K. Higai, T. Sasaki, Y. Asada, S. Ohshima and K. Koike, *Bioorg. Med. Chem. Lett.*, 2013, **23**, 5836–5839.

11 G. Yoon, W. Lee, S. N. Kim and S. H. Cheon, *Bioorg. Med. Chem. Lett.*, 2009, **19**, 5155–5157.

12 (a) J. Li, L. Pan, Y. Deng, U. Munoz-Acuna, C. Yuan, H. Lai, H. Chai, T. E. Chagwedera, N. R. Farnsworth, E. J. C. Blanco, C. Li, D. D. Soejarto and A. D. Kinghorn, *J. Org. Chem.*, 2013, **78**, 10166−10177. (b) X. Qiao, C. F. Liu, S. Ji, X. H. Lin, D. A. Guo and M. Ye, *Planta Med.*, 2014, **80**, 237−242.

13 M. M. Rahman, S. D. Sarker, M. Byres and A. I. Gray, *J. Nat. Prod.*, 2004, **67**, 402−406.

14 (a) X. Lin, S. Ji, X. Qiao, H. Hu, N. Chen, Y. Dong, Y. Huang, D. Guo, P. Tu and M. Ye, *J. Org. Chem*., 2013, **78**, 11835−11848. (b) A. León, J. A. Cogordán, O. Sterner and G. Delgado, *J. Nat. Prod*., 2012, **75**, 859−864.

15 *Sybyl Software*, version X 1.1; Tripos Associates Inc., St. Louis, MO, 2010.

16 X. Qiao, R. An, Y. Huang, S. Ji, L. Li, Y. Tzeng, D. A. Guo and M. Ye, *J. Chromatogr. A*, 2014, **1358**, 252−260.

17 (a) Y. Shi, Y. Liu, Y. Li, L. Li, J. Qu, S. Ma and S. Yu, *Org. Lett*., 2014, **16**, 5406−5409. (b) J. F. Xu, H. J. Zhao, X. B. Wang, Z. R. Li, J. Luo, M. H. Yang, L. Yang, W. Y. Yu, H. Q. Yao, J. G. Luo and L. Y. Kong, *Org. Lett*., 2014, **17**, 146−149.

18 T. Fukai, Q. H. Wang, T. Kitagawa, K. Kusano, T. Nomura and Y. Iitaka, *Heterocycles*, 1989, **29**, 1761−1772.

19 (a) R. D. H. Murray and M. M. Ballantyne, *Tetrahedron*, 1970, **26**, 4473−4479. (b) C. Ito, K. Fujiwara, M. Kajita, M. Ju-ichi, Y. Takemura, Y. Suzuki, K. Tanaka, M. Omura and H. Furukawa, *Chem. Pharm. Bull.*, 1991, **39**, 2509–2513. (c) N. Vera, A. Bardón, C. A. N. Catalán, T. E. Gedris and W. Herz, *Planta Med.*, 2001, 67, 674–677. (d) W. C. Lai, Y. T. Tsui, A. N. B. Singab, M. El-Shazly, Y. C. Du, T. L. Hwang, C. C. Wu, M. H. Yen, C. K. Lee, M. F. Hou, Y. C. Wu and F. R. Chang, *Int. J. Mol. Sci*., 2013, **14**, 15578−15594. (e) H. Li, M. Yang, J. Miao and X. Ma, *Magn. Reson. Chem*., 2008, **46**, 1203–1207. (f) Y. L. Huang, P. Y. Yeh, C. C. Shen and C. C. Chen, *Phytochemistry*, 2003, **64**, 1277−1283.

20 G. Yoon, W. Lee, S. N. Kim and S. H. Cheon, *Bioorg. Med. Chem. Lett*., 2009, **19**,

5155–5157.

21 T. Bruhn, Y. Hemberger, A. Schaumlöffel and G. Bringmann, *SpecDis*, version 1.51; University of Wuerzburg, Germany, 2011.

22 M. J. Frisch, G. W. Trucks, H. B. Schlegel, G. E. Scuseria, M. A. Robb, J. R. Cheeseman, G. Scalmani, V. Barone, B. Mennucci, G. A. Petersson, H. Nakatsuji, M. Caricato, X. Li, H. P. Hratchian, A. F. Izmaylov, J. Bloino, G. Zheng, J. L. Sonnenberg, M. Hada, M. Ehara, K. Toyota, R. Fukuda, J. Hasegawa, M. Ishida, T. Nakajima, Y. Honda, O. Kitao, H. Nakai, T. Vreven, J. A. Montgomery, J. E. Peralta, F. Ogliaro, M. Bearpark, J. J. Heyd, E. Brothers, K. N. Kudin, V. N. Staroverov, R. Kobayashi, J. Normand, K. Raghavachari, A. Rendell, J. C. Burant, S. S. Iyengar, J. Tomasi, M. Cossi, N. Rega, N. J. Millam, M. Klene, J. E. Knox, J. B. Cross, V. Bakken, C. Adamo, J. Jaramillo, R. Gomperts, R. E. Stratmann, O. Yazyev, A. J. Austin, R. Cammi, C. Pomelli, J. W. Ochterski, R. L. Martin, K. Morokuma, V. G. Zakrzewski, G. A. Voth, P. Salvador, J. J. Dannenberg, S. Dapprich, A. D. Daniels, O. Farkas, J. B. Foresman, J. V. Ortiz, J. Cioslowski and D. J. Fox, *Gaussian 09*, revision B.01; Gaussian Inc.: Pittsburgh, PA, 2010.

Table 1. ^{1}H (400 MHz) and ^{13}C (100 MHz) NMR data for **1**–**4** in DMSO-d_6.

	1		**2**		**3**[a]		**4**	
C	δ_C, type	δ_H (J in Hz)	δ_C, type	δ_H (J in Hz)	δ_C, type	δ_H (J in Hz)	δ_C, type	δ_H (J in Hz)
2	159.6, C		159.6, C		159.3, C		150.2, C	
3	119.1, C		119.2, C		101.2, C		100.1, CH	7.03, s
4	136.6, CH	7.86, s	136.6, CH	7.86, s	157.1, C		152.3, C	
5	156.8, C		156.8, C		156.9, C		89.1, CH	6.31, s
6	90.5, CH	6.49, s	90.5, CH	6.50, s	91.4, CH	6.67, s	156.7, C	
7	162.0, C		162.0, C		162.3, C		110.8, C	
8	113.3, C		113.3, C		114.6, C		149.1, C	
9	150.7, C		150.5, C		150.5, C		113.4, C	
10	103.6, C		103.7, C		96.9, C			
16	113.6, C		113.6, C		114.0, C		109.0, C	
20	155.9, C		156.0, C		155.7, C		155.4, C	
35	102.6, CH	6.35, d (2.0)	102.7, CH	6.35, d (2.4)	98.5, CH	7.12, d (2.4)	102.9, CH	6.45, d (2.0)
4.	158.3, C		158.3, C		156.8, C		158.1, C	
55	106.2, CH	6.25, dd (2.0, 8.4)	106.2, CH	6.25, dd (2.4, 8.4)	114.2, CH	6.94, dd (2.4, 8.4)	107.1, CH	6.37, dd (2.0, 8.4)
6(	131.4, CH	7.05, d (8.4)	131.4, CH	7.05, d (8.4)	120.3, CH	7.70, d (8.4)	126.4, CH	7.58, d (8.4)
2.	90.0, CH	4.52, q (6.8)	93.9, CH	4.39, dd (4.8, 6.8)	90.2, CH	4.57, q (6.6)	89.0, CH	4.45, q (6.8)
3.	43.2, C		42.7, C		43.7, C		43.1, C	
4″	14.1, CH_3	1.35, d (6.8)	59.6, CH_2	3.75, m	14.1, CH_3	1.37, d (6.6)	14.2, CH_3	1.34, d (6.8)
[b]5″	25.3, CH_3	1.21, s	26.5, CH_3	1.29, s	25.2, CH_3	1.23, s	25.8, CH_3	1.21, s
[b]6″	21.1, CH_3	1.47, s	20.8, CH_3	1.54, s	21.0, CH_3	1.51, s	21.7, CH_3	1.51, s
OCH_3	56.4, CH_3	3.85, s	56.4, CH_3	3.86, s	56.8, CH_3	3.98, s	55.6, CH_3	3.82, s
OH		9.37, s		9.39, br s		9.99, s		10.51, br s
		9.33, s		9.39, br s				9.54, br s
				4.99, br s				

[a]Data were recorded at 600 MHz for ^{1}H NMR and 150 MHz for ^{13}C NMR;

[b]The assignments are interchangeable.

Table 2. PTP1B inhibitory and cytotoxicity data (IC_{50} values, μM) for (2″*R*)-**1**, (2″*S*)-**1** and racemic **2**–**4**.

Compounds	PTP1B	SW480	HepG2	A549
(2″*R*)-**1**	12.1	11.6	23.8	40.0
(2″*S*)-**1**	13.6	> 40	> 40	> 40
2	10.3	> 40	> 40	> 40
3	13.5	> 40	> 40	> 40
4	2.2	4.4	6.7	13.7
[a]Ursolic acid	6.2	N.A.	N.A.	N.A.

[a]Positive control. N.A., not available.

Figure legends

Fig. 1. Structures of **1**, (2″*R*)-**1**, (2″*S*)-**1** and **2**–**4**.

Fig. 2. Key HMBC and NOE correlations for **1** and **4**.

Fig. 3. Comparison of the calculated ECD spectra for (2″*R*)-**1** and (2″*S*)-**1** with the experimental ECD spectra for racemic **1**, (2″*R*)-**1** and (2″*S*)-**1**.

Fig. 4. X-ray structures of racemic **1**, (2″*R*)-**1** and (2″*S*)-**1**.

Fig. 5. Chiral separation of racemic **1**–**4** by SFC.

Fig. 6. Chiral separation of racemic **1** and purity analysis of (2″*R*)-**1** and (2″*S*)-**1** by normal-phase HPLC.

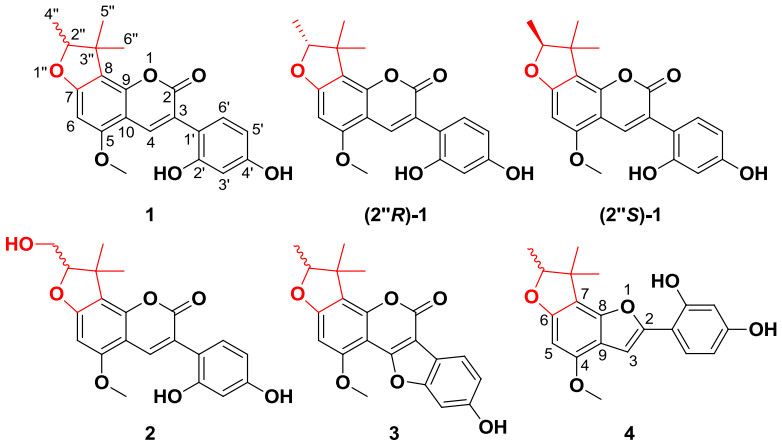

Fig. 1. Structures of **1**, (2″*R*)-**1**, (2″*S*)-**1** and **2**–**4**.

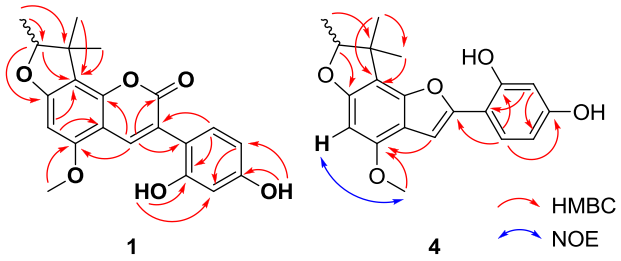

Fig. 2. Key HMBC and NOE correlations for **1** and **4**.

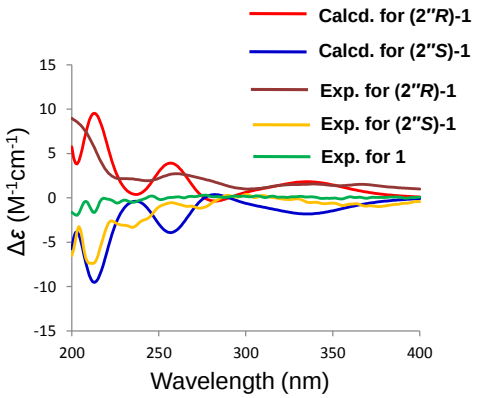

Fig. 3. Comparison of the calculated ECD spectra for (2″*R*)-**1** and (2″*S*)-**1** with the experimental ECD spectra for racemic **1**, (2″*R*)-**1** and (2″*S*)-**1**.

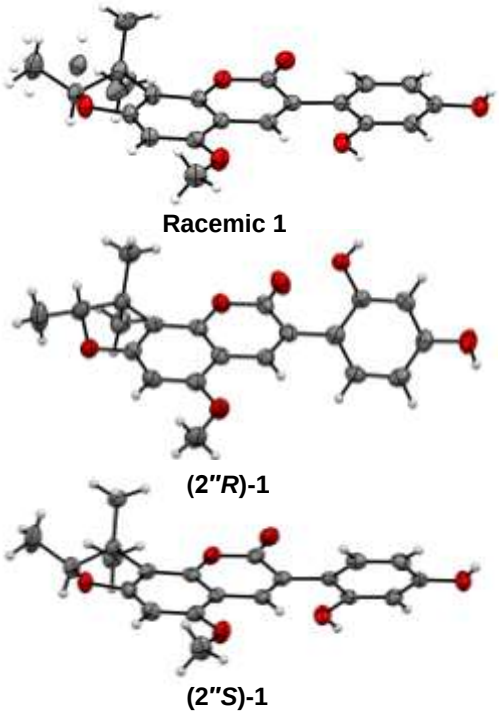

Fig. 4. X-ray structures of racemic **1**, (2″*R*)-**1** and (2″*S*)-**1**.

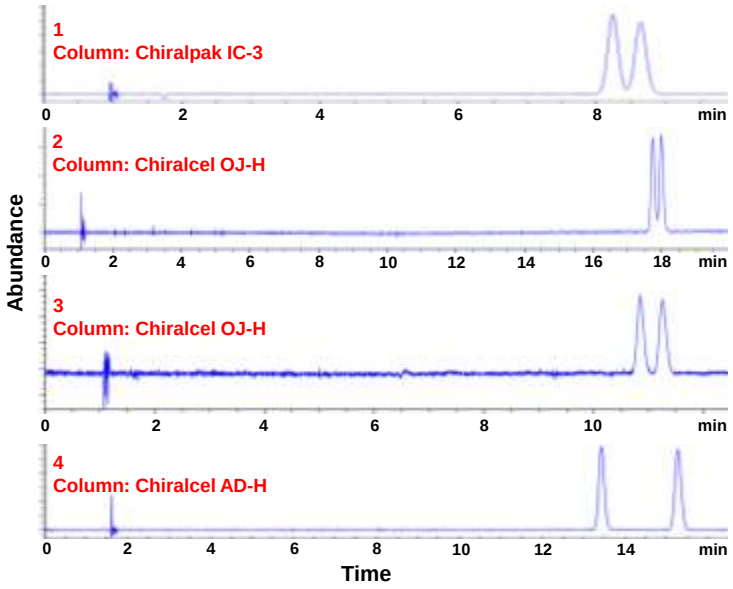

Fig. 5. Chiral separation of racemic **1**–**4** by SFC.

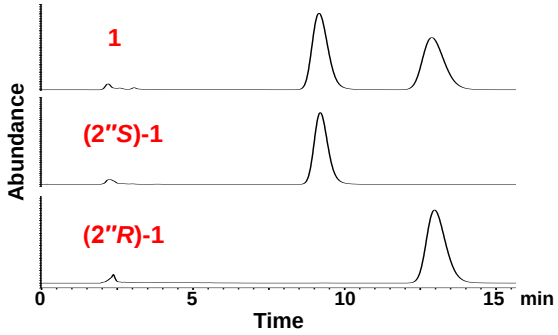

Fig. 6. Chiral separation of racemic **1** and purity analysis of (2″*R*)-**1** and (2″*S*)-**1** by normal-phase HPLC.

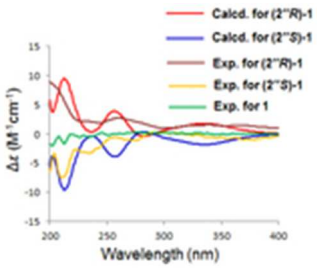

13x11mm (300 x 300 DPI)

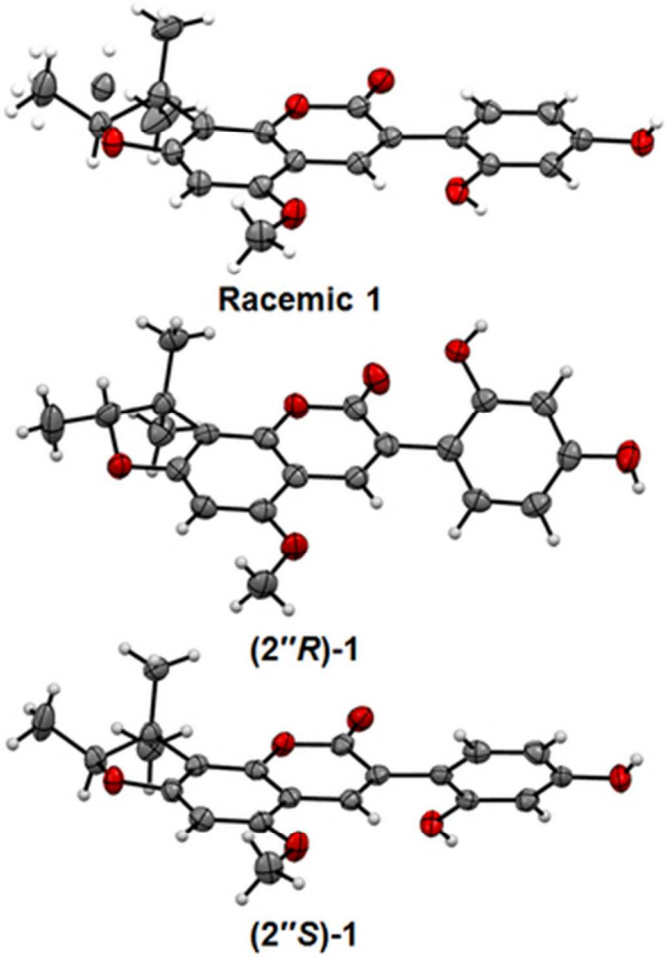

29x41mm (300 x 300 DPI)

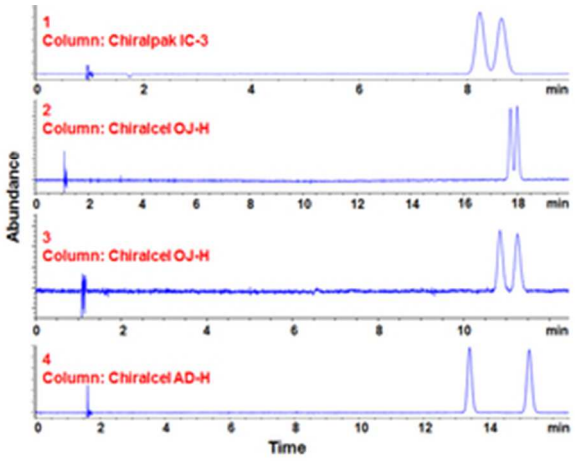

24x19mm (300 x 300 DPI)

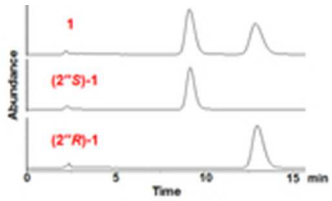

14x8mm (300 x 300 DPI)